

Photoinduced Formation of N₂ Molecules in Ammonium Compounds

Emad F. Aziz,[†] Johan Gråsjö,[‡] Johan Forsberg,[§] Egil Andersson,[§] Johan Söderström,[§] Laurent Duda,[§] Wenhua Zhang,^{||,⊥} Jinglong Yang,[⊥] Stefan Eisebitt,[†] Christel Bergström,[‡] Yi Luo,^{||} Joseph Nordgren,[§] Wolfgang Eberhardt,[†] and Jan-Erik Rubensson^{*,†,§}

BESSY, Albert-Einstein Str. 15, D-12489 Berlin, Germany, Department of Pharmacy, Uppsala University, P.O. Box 580, SE-751 23 Uppsala, Sweden, Department of Physics, Uppsala University, Box 530, SE-751 21 Uppsala, Sweden, Theoretical Chemistry, Royal Institute of Technology, Teknikringen 36, SE-100 44, Stockholm, Sweden, and Hefei National Laboratory of Physical Sciences at the Microscale, University of Science and Technology of China, Hefei, Anhui 230026, China

Received: May 11, 2007; In Final Form: July 17, 2007

Via fluorescence yield (FY) and resonant inelastic scattering spectroscopy in the soft X-ray range we find that soft X-rays induce formation of N₂ molecules in solid NH₄Cl and in related compounds. The nitrogen molecules form weak bonds in NH₄Cl, so that a substantial fraction of the molecules remains in the sample. From measurements of the FY as a function of exposure and temperature, the rates for the photochemical processes are estimated. At elevated temperatures (363 K), several nitrogen atoms are removed from the sample per incoming photon. At lower temperatures (233 K), the rate is reduced to around 0.02 nitrogen atoms for each incoming photon. Virtually all these atoms form N₂ molecules which are bound in the sample. The generality and implications of these results are briefly discussed.

Introduction

The balance between nitrogen atoms in the form of inert N₂ and as a constituent in reactive amino molecules is crucial in the development of planetary atmospheres¹ and in creating the prerequisites for biological processes.² Today, the production of synthetic nitrogen fertilizer from atmospheric N₂, necessary to provide the population with protein food, has resulted in a significant anthropogenic influence on the global nitrogen cycle: the increased nitrogen fixation is an environmental problem.³ The understanding of processes where nitrogen in one form is transferred to the other has therefore special interest.

Radiation damage is a notorious problem both in X-ray crystallography and spectroscopy. It is usually assumed that radiation damage is nonspecific so that spectra are contaminated and diffraction patterns blurred. On the other hand, it has been demonstrated that radiation in certain cases can induce new specific structures which can be studied in X-ray crystallography,⁴ and the influence on X-ray absorption spectra of particular photoinduced processes in liquids has recently attracted attention.^{5,6}

VUV and X-ray radiation are known to cause defects in ammonium halides at low temperatures and doses. In NH₄Cl formation of Cl₂⁻ ions (V_k centers)⁷ and NH₃Cl, color centers⁸ have been observed and defects initially assigned to anion vacancies (F centers)⁹ have been identified as interstitial hydrazine (N₂H₄⁺) ions¹⁰ occupying initial ammonium sites.

Here we show that soft X-ray radiation efficiently induces N₂ formation in NH₄Cl. The N₂ molecules prevail in the solid

and make up a substantial part of the exposed sample. A similar behavior is found in NH₆PO₄, demonstrating that such photochemical N₂-forming reactions are not restricted to ionic NH₄⁺ compounds and suggesting that such reactions may be common in nitrogen-containing compounds.

Experimental Methods

Soft X-ray fluorescence yield (FY) spectra were measured at the nitrogen *K* edge using a GaAsP photodiode with 25 mm² active area in the LIQUIDROM endstation¹¹ at beamline UE41-PGM¹² at BESSY, Berlin. The synchrotron radiation impinged on the sample in normal incidence, and the detector measured radiation in a direction 35° off normal in the polarization plane of the incoming photons. For NH₄Cl, FY as a function of exposure at various photon energies in the 190–1500 eV range was measured at 233, 298, and 363 K. The average intensity of the incoming beam varied in the 5 × 10¹⁴ to 1 × 10¹⁶ photons/s/cm² range, whereas due to the time structure of the synchrotron radiation the peak intensity was around 50 times higher. No nonlinear effects in the dose dependence were observed. Samples were prepared in the form of tablets, in the form of powder pressed into indium foils, and in the form of crystals grown from aqueous solutions. The various preparation methods gave consistent results. Dose-dependent FY spectra were also measured for ammonium iodide (NH₄I), ammonium phosphate (NH₆PO₄), and *l*-alanine (C₃H₇O₂N).

Resonant inelastic soft X-ray scattering (RIXS) spectra of NH₄Cl were measured in a grazing incidence spectrometer¹³ at beamline I511¹⁴ at MAX-II, Lund, where also FY spectra were monitored using a multichannel plate detector.

Theoretical Calculations

Calculations for NH₄Cl crystals were carried out using the local-orbital density-functional method implemented in the DMOL³ package¹⁵ with double numerical plus polarization basis

* Corresponding author. E-mail: emad@bessy.de, jan-erik.rubensson@fysik.uu.se.

[†] BESSY.

[‡] Department of Pharmacy, Uppsala University.

[§] Department of Physics, Uppsala University.

^{||} Royal Institute of Technology.

[⊥] University of Science and Technology of China.

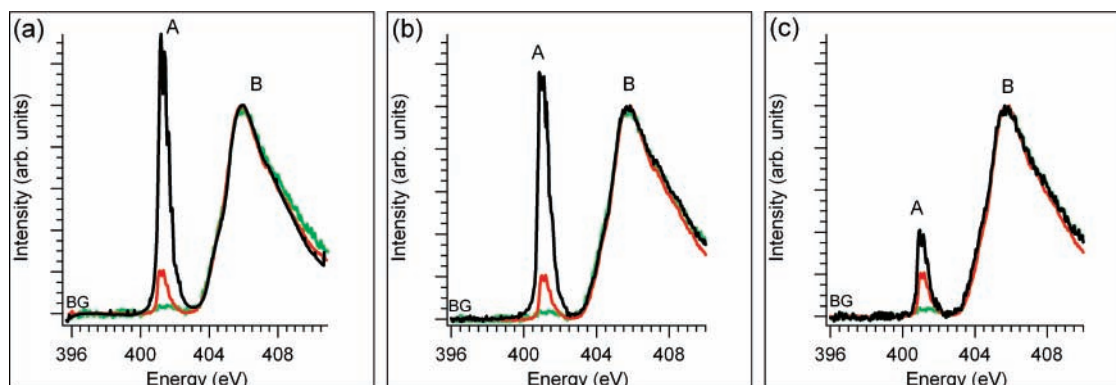


Figure 1. FY spectra of solid NH₄Cl, for a pristine sample measured in a fast (3 min) scan (green), in a 12 min scan (red), and measured after longer exposure to synchrotron radiation (black) at (a) 233 K, (b) 298 K, and (c) 363 K.

set and the generalized gradient approximation.¹⁶ The Monkhorst-Pack special k-points scheme¹⁷ was used with $7 \times 7 \times 7$ k-points sampling for the structure optimization, which were performed for the ground and electronically excited states.

Soft X-ray absorption spectra of N_xH_y species were calculated using the gradient-correlated density-functional theory implemented in the DeMon code.¹⁸ The iglo-iii basis set of Kutzelnigg, Fleischer, and Shindler¹⁹ is used for the excited nitrogen, while a five-electron effective core potential (ECP)¹⁸ was used to describe the non-excited nitrogen atoms. A Gaussian function (fwhm = 0.3 eV) is used for convoluting the spectra below the ionization potential (IP), while a Stieltjes imaging approach is used to describe the spectra above the IP in the continuum.

Results

Figure 1 shows the FY as a function of the energy of the incoming photons, E_1 , of the NH₄Cl crystal before and after exposure to synchrotron radiation at various energies and temperatures. All spectra show a sharp peak (A) with a maximum at 401.05 eV and a broader structure (B) with a maximum at 405.75 eV. In general, the A/B intensity ratio increases with exposure, and it becomes largest at high exposure and low temperature. Similar results were obtained independent of photon energies in the range from 190 eV, below the Cl *L* absorption edge, to 1500 eV, far above the N *K* edge. Excitation at resonances just above the Cl *L* and N *K* edges did also not appreciably influence the dose dependence of the spectra. Although the relative intensities of the A and B features are dose- and temperature-dependent, their individual spectral shape does not change, either as a function of exposure or as a function of temperature in the 233–363 K range.

Figure 2 shows the FY signal as a function of the number of incoming photons, n , at fixed $E_1 = 405.75$ eV (top), 401.05 eV (middle), and 395.75 eV (bottom), corresponding to the features B, A, and the background level (BG), respectively. The general trend is that the background is slightly increasing with exposure at low temperatures, and that this increase becomes much more dramatic at 363 K. The signal corresponding to the A feature increases from the background value, and the rise seems slightly temperature-dependent. The signal corresponding to the B feature decreases monotonically with exposure, and it is also temperature-dependent. On the basis of these spectral variations we will identify the principal photochemical processes and estimate their rates in the Discussion section.

In Figure 3 (top), the FY spectrum of the NH₄Cl is compared to the soft X-ray absorption spectrum of gas-phase N₂.²⁰ The peak around 401 eV, assigned to the $1s \rightarrow 1\pi^*$ excitation in gaseous N₂ virtually coincides with the A feature in the NH₄Cl

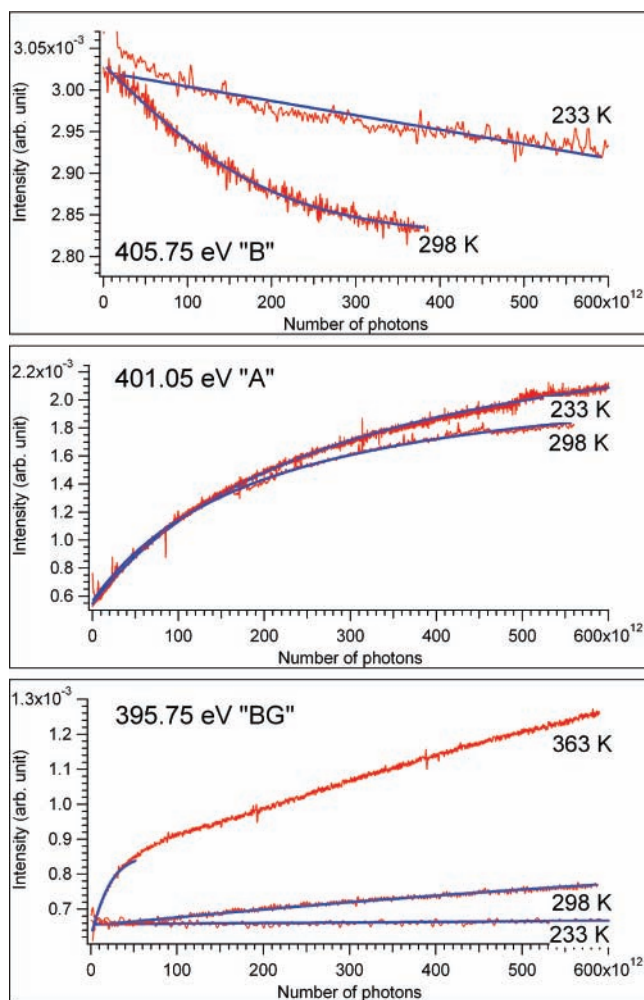


Figure 2. The dependence of the FY signal excited at 395.75 eV (bottom), 401.05 eV (middle), and 405.75 eV (top) on exposure to soft X-ray photons, recorded at 233 and 298 K. The intensity dependence of the background is also shown at 363 K. See Discussion section for an explanation of the (blue) fitted curves.

spectrum, even reproducing details in the vibrational fine structure. In Figure 4 (bottom), we demonstrate that inelastic scattering spectra, resonantly excited at the A feature, also are similar to the corresponding RIXS spectra of gas-phase N₂.²¹ At higher excitation energies, corresponding to the B feature in the FY spectrum, the RIXS spectra completely change character, and they are dominated by two broad structures with maxima around 390 and 395 eV. In Figure 4, we show a blow-up of the region where this change occurs. Spectra numbered

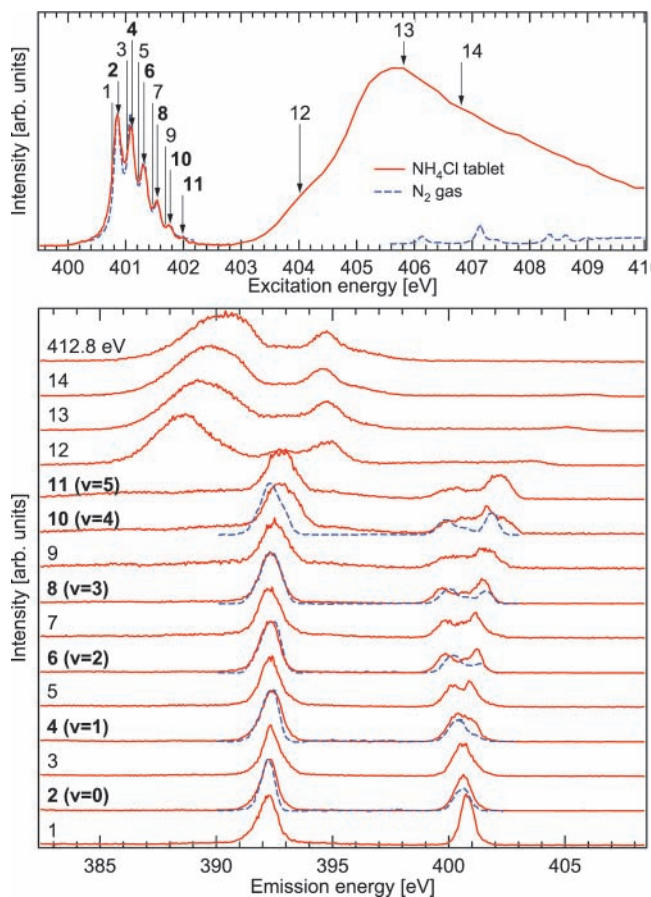


Figure 3. The FY spectrum of an exposed NH_4Cl tablet, compared to the gas-phase absorption spectrum of N_2 from ref 20 (top). RIXS spectra (below) excited at energies indicated by numbers in the FY spectrum compared to RIXS spectra of gas-phase N_2 from ref 21.

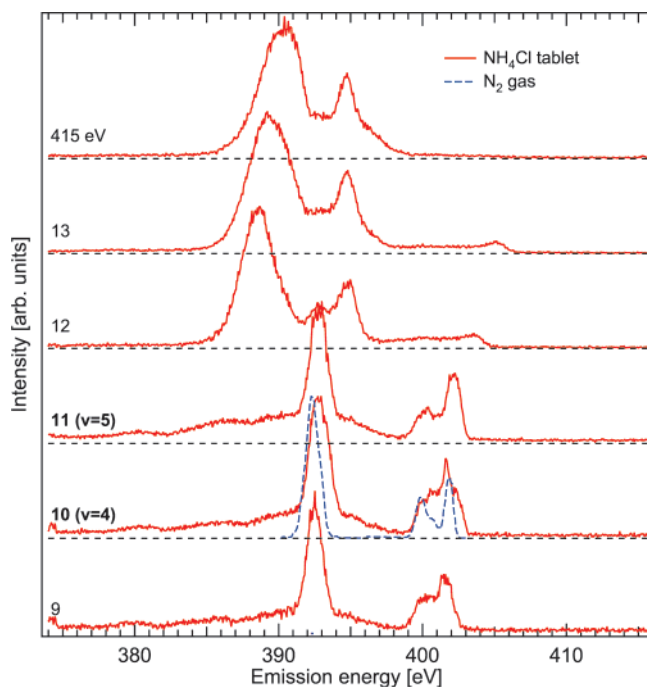


Figure 4. RIXS spectra excited in the energy range where substantial deviations from the gas-phase spectrum are observed.

10 and 11 are excited at the high end of the A feature, corresponding to the vibrational quantum number $v = 4$ and 5 of the gas-phase $1s \rightarrow 1\pi^*$ resonance. Apart from the rather sharp structures which are seen also in the gas-phase spectrum,

there is extended intensity spread out over a large energy region. Again, spectra excited at the B feature show a completely different character.

In Figure 5, FY spectra of some related nitrogen-containing compounds are shown for comparison. The spectrum of NH_4I (Figure 5a) is dominated by a rather broad structure with a maximum just below 406 eV, similar to feature B in the NH_4Cl spectrum. The spectral shape changes only slightly with exposure, and no measurable counterpart to the A feature in the NH_4Cl spectrum appears. As is seen in Figure 6, however, the photon beam has a violent impact on the ammonium iodide; the FY signal excited at resonance decreases by a factor of 3 after exposure to 10^{16} photons. The background does not vary much during the first 4×10^{15} photons but then it decreases rapidly. The FY spectrum of ammonium phosphate, NH_6PO_4 , (Figure 5b) also bears similarities to the NH_4Cl spectrum where the B feature is narrower and peaks just above 406 eV. The NH_6PO_4 spectrum also has a direct counterpart to the A feature, and the relative intensity of the two features are dose-dependent. In Figure 6b, we see that the dose dependence of the two features is in qualitative agreement with the dependence in NH_4Cl . The FY spectrum of *l*-alanine, $\text{C}_3\text{H}_7\text{O}_2\text{N}$, (Figure 5c) differs substantially from the spectra of the other compounds, and it shows complex dose dependence, with strong variation of the spectral features (Figure 6c) and no apparent feature corresponding to the A peak in NH_4Cl .

Discussion

On the basis of the evidence presented above, we assign the A peak in the NH_4Cl spectrum to $1s \rightarrow 1\pi^*$ transitions in N_2 molecules which are formed by the photon beam impact and prevail in the solid. The B feature we assign to transitions of an electron from the N $1s$ level to the first unoccupied states in NH_4Cl . The constant spectral shape indicates that this peak represents the undistorted NH_4Cl sample, and the dose-dependent overall decrease in intensity indicates that the number of nitrogen atoms in this chemical form decreases.

To estimate the rates for these photochemical processes, we describe the dose dependence of the FY signal in terms of a simple model. We assume a two-step process, where core-hole states are excited by the incoming radiation and the measured fluorescence is generated as these states subsequently decay. As these processes are crucially dependent on the chemical surrounding of the atoms, we can relate the FY intensity to the number of atoms in this specific surrounding. Virtually all impinging soft X-ray photons are absorbed in the sample, where there is a competition between various processes leading to the absorption of a photon and eventually to the emission of a secondary photon. This photon may then be reabsorbed in the sample, so that the FY intensity is dependent on the absorption cross section both for primary and secondary photons. Assuming that there is no inherent angular anisotropy on the atomic scale, one gets a simple expression for the FY intensity as a function of incoming energy, E_1 :²³

$$I(E_1) \propto \sum_i \frac{\mu_i(E_1)\omega_i}{\mu(E_1) + 0.82\mu(E_{2,i})} \quad (1)$$

where μ is the absorption coefficient [cm^{-1}], μ_i is the absorption coefficient related to excitations of specific states with branching ratio ω_i for emitting a photon with energy $E_{2,i}$, that can be detected in our detector. The factor 0.82 comes from geometric considerations for our experimental setup.

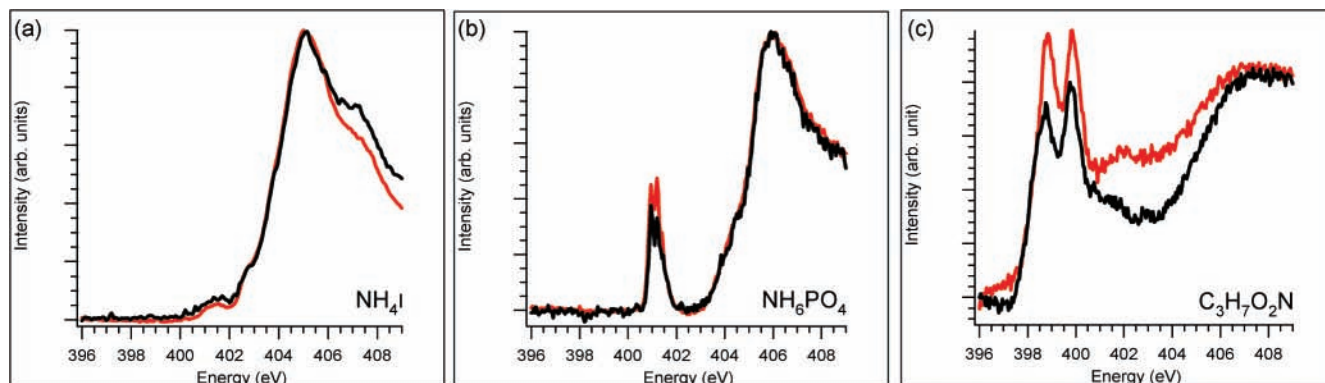


Figure 5. FY spectra of (a) ammonium iodide, (b) ammonium phosphate, and (c) *l*-alanine measured before (red) and after (black) exposure to soft X-rays.

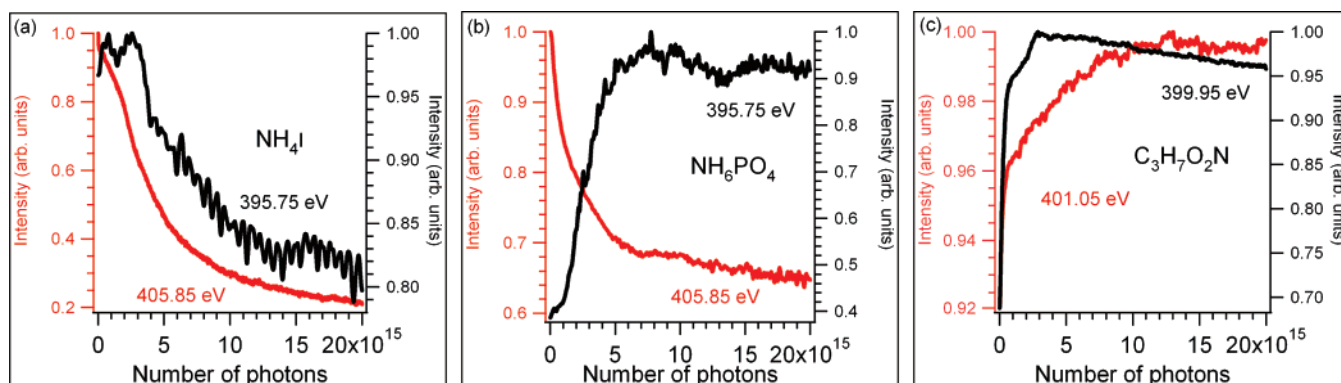


Figure 6. The dose dependence at room temperature of the FY intensity of (a) ammonium iodide, (b) ammonium phosphate, and (c) *l*-alanine at some chosen excitation energies.

First we turn our attention to the exposure dependence when the energy of the incoming photons is tuned to the B resonance (Figure 2, top). We assume that the intensity at $E_1 = 405.75$ eV is dominated by the N 1s excitations, that is, that $\mu_i(E_1)\omega_i$ is small for all other excitations. This determines $E_{2,i}$ since we see in Figures 3–4 that the N K fluorescence falls in the 385–400 eV region. Assuming (as in ref 23) that $\mu_i(E_1) \approx \mu_B(E_1) + \mu(E_{2,B})$, where we let $i = B$ indicate association with the excitation responsible for the B resonance, and neglecting any dose dependence of the branching ratio for radiative decay, we get the approximate dependence on the absorption coefficients:

The absorption coefficient can be written as follows:

$$I_B(E_1) \propto \frac{\mu_B(E_1)}{\mu_B(E_1) + 1.82\mu(E_{2,B})} \quad (2)$$

$$\mu_i = \frac{N_i}{V} \sigma_i \quad (3)$$

where σ_i [cm²/atom] is the atomic cross section associated with the specific excitation, and N_i is the number of available atoms for this excitation in the exposed volume, V . At the B resonance ($E_1 = 405.75$ eV), we let $N_i = N_B$, and assume that the dose variation is dominated by changes in the atomic density N_B/V . The self-absorption of the emitted radiation ($E_{2,B} = 385$ –400 eV) is dominated by Cl 2p absorption so that $\mu(E_{2,B}) \approx N_{Cl}/V\sigma_{Cl}(E_{2,B})$. If λ_B is the number of atoms removed from the initial chemical surrounding per photon which is absorbed in the volume, V , we assume that

$$\frac{dN_B}{dn} = -\lambda_B N_B \quad (4)$$

where n is the number of photons. For eq 4 strictly to hold, the probed volume must be the same during the exposure, an approximation which is good at small λ_B . Equation 4 has the following solution:

$$N_B(n) = N_{0,B} e^{-\lambda_B n} \quad (5)$$

where $N_{0,B}$ is the number of initially exposed atoms. Combining eqs 2, 3, and 5, we get for the photon exposure dependence of the intensity of the B peak:

$$I_B(n) \approx I_B(0) \frac{N_{0,B} e^{-\lambda_B n}}{N_{0,B} e^{-\lambda_B n} + 1.82 N_{Cl} \frac{\sigma_{Cl}(E_{2,B})}{\sigma_B(E_1)}} \quad (6)$$

where the ratio of the atomic cross sections [$\sigma_{Cl}(E_{2,B})/\sigma_B(E_1)$] can be estimated from ref 24 and the measured absorption spectrum to be 0.6. Since $N_{0,B} = N_{Cl}$ we get

$$I_B(n) \approx I_B(0) \frac{e^{-\lambda_B n}}{e^{-\lambda_B n} + 1.1} \quad (7)$$

This function is able to fit the measured curves in Figure 2 (top) with λ_B as parameter well. At 298 K, the fit result is λ_B (298 K) = 9.2×10^{-15} atoms/photon. The beam spot size is $250 \times 70 \mu\text{m}$, and the penetration length is roughly $0.2 \mu\text{m}$.²⁴ With a lattice parameter of 3.891 \AA ,²² we estimate that $N_{0,B} \approx 6 \times 10^{13}$ atoms. Thus, our model implies that a photon hitting the sample will remove a nitrogen atom from its initial NH₄Cl chemical surrounding with more than 50% probability. At 233 K, the fit results in λ_B (233 K) = 3.3×10^{-16} atoms/photon, that is, a reduction of almost a factor of 30.

If all the nitrogen atoms which are removed from the initial NH_4Cl chemical surrounding react to form adsorbed N_2 molecules, we would have for the number of N atoms in molecular form

$$N_A(n) = N_{0,B}(1 - e^{-\lambda_B n}) \quad (8)$$

and the dose dependence of the signal excited at 401.05 eV would be

$$I_A(n) \approx I_A(\infty) \frac{N_{0,B}(1 - e^{-\lambda_B n})}{N_{0,B}(1 - e^{-\lambda_B n}) + 1.82N_{\text{Cl}} \frac{\sigma_{\text{Cl}}(E_{2,B})}{\sigma_A(E_1)}} \quad (9)$$

where $\sigma_A(E_1)$ is the atomic cross section for the $1s \rightarrow \pi^*$ resonance in N_2 , which we estimate to be about 5 times larger than the atomic cross section corresponding to the B resonance in NH_4Cl , and thus the $\sigma_{\text{Cl}}(E_{2,B})/\sigma_A(E_1)$ ratio is estimated to be 0.12. Hence

$$I_A(n) \approx I_A(\infty) \frac{(1 - e^{-\lambda_B n})}{(1 - e^{-\lambda_B n}) + 0.22} \quad (10)$$

This equation fits the experimental curves in Figure 2 (middle) well. We obtain $\lambda_B(298 \text{ K}) = 1.0 \times 10^{-15}$ atoms/photon, a value which is substantially smaller than the value fitted to the corresponding dose dependence of the B peak. The model implies that around 10% of the nitrogen atoms which are removed from the initial NH_4Cl chemical surrounding form N_2 molecules that are bound in the solid. Also, here the rate is temperature-dependent, and we get $\lambda_B(233 \text{ K}) = 6.8 \times 10^{-16}$ atoms/photon. Thus, the rate of formation of bound N_2 molecules decreases with temperature, albeit not as dramatic as the removal from the NH_4Cl chemical surrounding. At low temperatures, the fit according to the model gives an N_2 formation rate which is even larger than the N removal rate. This contradictory result reflects the limitations of the model, for example, it relies on the assumption that the number of chlorine atoms in the exposed volume is dose-independent. Thus, the fit results must be seen as estimates, and in this case the reasonable conclusion is that now most of the removed N atoms indeed form bound N_2 at low temperatures.

At excitation just below the N *K* edge, finally, the cross section is totally dominated by Cl 2p excitations so that $\mu_{\text{BG}}(E_1) \approx (N_{\text{Cl}}/V) \times \sigma_{\text{Cl}}(E_1)$. The energy of the photons generated in the decay falls just below the Cl 2p edge, $E_{2,\text{BG}} < 200$ eV, where the photoabsorption cross section is determined by non-resonant excitation of electrons in states derived from N 2s/2p and Cl 3s/3p orbitals. Using ref 24 we estimate that $\mu(E_{2,\text{BG}}) \approx (N_{\text{Cl}}/V + 0.51 \cdot N_{\text{N}}/V) \times \sigma_{\text{Cl}}(E_{2,C})$, and that $\sigma_{\text{Cl}}(E_{2,\text{BG}})/\sigma_{\text{Cl}}(E_1) \approx 3.85$. If we neglect the H atoms, we thus have for the background intensity ($E_1 = 395.75$ eV):

$$I_{\text{BG}}(n) \approx \frac{N_{\text{Cl}}}{N_{\text{Cl}} + 0.82(N_{\text{Cl}} + 0.51N_{\text{N}}) \times 3.85} \approx \frac{N_{\text{Cl}}}{4.16N_{\text{Cl}} + 1.58N} \quad (11)$$

Assuming that the Cl atoms remain in the volume, any dose dependence in the signal is due to N atoms desorbing or diffusing away from the probed volume. We have

$$N_{\text{N}}(n) = N_{0,B} e^{-\lambda_D n} \quad (12)$$

where λ_D is the rate at which the N atoms disappear from the volume per incoming photon. Since $N_{0,B} = N_{\text{Cl}}$, we have

$$I_{\text{BG}}(n) \approx I_{\text{BG}}(0) \frac{1}{4.16 + 1.58e^{-\lambda_D n}} \quad (13)$$

From the measurements (Figure 2, bottom) we see that the background intensity is almost constant at the lowest temperature. From the fit we get $\lambda_D(233 \text{ K}) = 9.4 \times 10^{-17}$ atoms/photon. Already at 298 K there is a clear positive slope, and the fit result is $\lambda_D(298 \text{ K}) = 1.4 \times 10^{-15}$ atoms/photon. This indicates that a substantial fraction of the N atoms removed from the initial NH_4Cl chemical surrounding indeed leave the probed volume, but that this fraction is much smaller at low temperatures. At 363 K, the increase in signal is steep and it is not possible to reasonably fit eq 13 to the whole curve. Fitting the first part of the curve (Figure 2, bottom) gives $\lambda_D(363 \text{ K}) = 5.7 \times 10^{-14}$ atoms/photon. At this rate, 50% of the atoms in the initial volume would be removed already after 1.2×10^{13} photons, that is, the assumption made in eq 4 is not valid and the present model cannot be used to estimate the rates for the various processes at these high temperatures.

In summary, the simple models give the following picture. At room temperature, each photon hitting the sample removes a nitrogen atom from the initial NH_4Cl chemical surrounding with around 50% probability. At low temperature, the removal rate decreases by at least an order of magnitude. At room temperature, only a small fraction of the nitrogen atoms form N_2 molecules which are bound in the sample; however, at low temperatures, the majority of the removed nitrogen atoms take this form. At high temperatures, the rate of diffusion/desorption of atoms from the exposed volume is very high.

Below we briefly discuss some possible mechanisms for this behavior. It is unlikely that the N_2 -forming reaction proceeds without being mediated via intermediate species. As seen in Figure 1, the only dose dependence in the FY spectrum of NH_4Cl concerns the A/B intensity ratio, whereas the spectral shape of the two features remains unchanged. In Figure 7, we show that the formation of any intermediate species would give a specific fingerprint in the FY spectrum. Especially, any appreciable concentration of N_2H_4^+ , NH_2 , or NH_3 would be immediately reflected in the FY spectrum. The absence of any such signal is intriguing since it has been shown that VUV and X-ray radiation induce formation of hydrazine N_2H_4^+ (7) and NH_3Cl color centers (5b). The observation can be explained if these units are intermediate species and the last step in the N_2 -forming reaction is much faster than the first step(s). The fact that hydrazine derivatives in aqueous dispersions of TiO_2 efficiently produce N_2 gas under UV illumination²⁵ gives support for such an interpretation. This photocatalytic process is initiated when radiation creates electron-hole pairs in the TiO_2 catalyst. As soft X-rays create electron-hole pairs in NH_4Cl , it is conceivable that the compound itself takes the function of the catalyst for N_2 formation from initially photoinduced hydrazine ions. This suggested reaction path is by no means exclusive.

The vibronic coupling associated with electronic excitations is large in ionic compounds, especially when the excitation involves a change in the charge state of the ions. This is confirmed by X-ray emission spectroscopy where the vibrational energy associated with the fast nuclear relaxation occurring between excitation and emission can be several electronvolts.²⁶ Our calculations indicate that nitrogen core ionization does not induce dissociation of an NH_4^+ group. However, the core excitation from N 1s to the lowest unoccupied molecular orbital (LUMO) leads to a fast dissociation of an NH_4^+ group, and

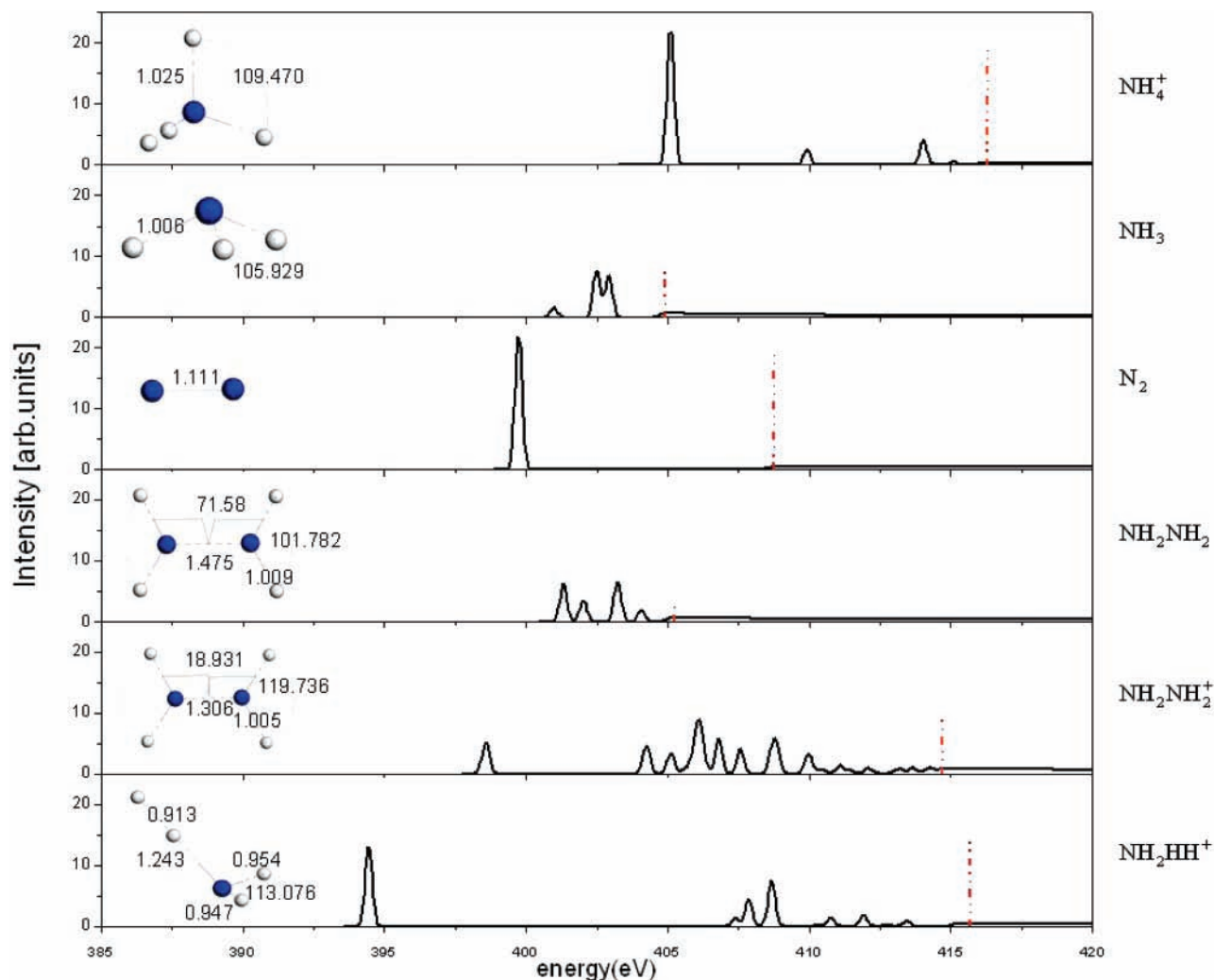


Figure 7. Calculated absorption spectra demonstrate the sensitivity to the nitrogen bonding. The experimental FY spectra do not show any traces of ammonia (second row) or hydrazine in neutral (fourth row) or ionic (fifth row) form, and also not of N atoms in the “NH₂” geometry (sixth row) predicted for the 1s → LUMO excited state.

similar behavior has also been found for the valence excitations, for instance, the highest occupied molecular orbital (HOMO) to LUMO+1 transition. The dissociation forms NH₂ radicals, which are also possible as intermediate species. After diffusion of the radicals through the material, N₂ may be formed in reactions of the type 2NH₂ → N₂ + 2H₂.

In a more general perspective, the energy transferred to the nuclear motion via vibronic coupling corresponds to high temperatures in the immediate vicinity of the excitation. It was shown early on that NH₄Cl sublimates in the form of HCl and NH₃ at elevated temperatures and low pressure,²⁷ and it is well-known that the 2NH₃ → N₂ + 3H₂ reaction is efficiently driven by catalytic mechanisms and elevated temperatures (at low pressures), and that it also can be photoinduced.²⁸ Thus, the soft X-rays simultaneously provide both a locally high temperature and the charges which are provided by the excitations of the catalyst in photocatalytic processes. Such a mechanism is general and suggests that similar processes may occur in a wide range of materials.

The results also indicate that the N₂ molecules are bound in the crystal. That the bond energy is weak is seen already in the resemblance with the gas-phase absorption spectrum (Figure 3), with resolved vibrational excitations up to $\nu = 5$. In case of chemisorption the distortion of the molecular absorption spectrum is much more pronounced,²⁹ and we can conclude from

the spectrum that the bonding is more similar to the case of physisorption.³⁰ Also the resemblance to the gas-phase RIXS spectrum is indicative of weak bonding. Apart from transitions back to the electronic ground state (around 400 eV in Figures 3 and 4), the RIXS transitions in gas-phase N₂ reach the 3 σ_g^{-1} 1 π_g a¹Π_g (around 392 eV) final state only, due to strict dipole selection rules.²¹ That the same appears to be true for the N₂ signal from the NH₄Cl sample indicates that there is no substantial symmetry breaking in the bound molecule. For isolated molecules, the spectral shape of each electronic transition is due to vibrational excitations, which are well described within the Kramers–Heisenberg formalism and the Franck–Condon model.²¹ For excitations around $\nu = 4$ and higher, we see additional broadening (Figure 4) in the spectra, and particularly, intensity is spread out in a large range from the peak at 392 eV and extends to below 385 eV. The spectra indicate continuous energy losses of up to more than 15 eV. This cannot be explained in terms of excitations in a free N₂ molecule. We believe that this smeared-out intensity can be related to interactions between the molecule and the solid. Dissipation of vibrational energy, and corresponding energy losses, may be expected considering the high density of light hydrogen atoms and the ionic nature of the initial compound. The interaction with the solid would most strongly influence the population of the 3 σ_g^{-1} 1 π_g a¹Π_g final state because here

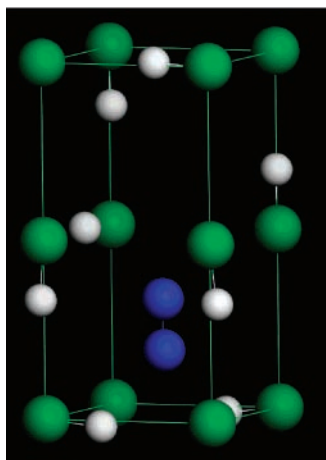


Figure 8. Optimized geometry, where the nitrogen molecule (blue) is bound in a dipole well constituted by the chlorine (green) and hydrogen (white) atoms.

the N–N equilibrium distance is longer and the potential curve is much shallower than in both the ground state and the core excited state. The width of the corresponding spectral feature is significantly larger than what is expected for a free molecule.

However, we cannot rule out a contribution to the smeared-out intensity in these spectra from scattering to final valence-hole-conduction-band-electron states in the (intact or distorted) NH_4Cl crystal. In principle this is possible also when the excitation energy is detuned several electronvolts below the threshold for the corresponding resonances. Therefore, the RIXS data do not give an unambiguous indication of the interaction between the molecule and the solid.

The temperature dependence gives evidence of a weak bond with energies in the order of $kT \approx 25$ meV.

Assuming the N_2 is generated within the crystal, we have optimized the geometry of N_2 in two unit cells, for which 12 Cl atoms are fixed in their crystal positions and the N_2 and H atoms are fully relaxed in space. The final geometry is shown in Figure 8. It is noted that for a neutral system, N_2 is slightly unstable in the dipole well with a binding energy of -6.02 kcal/mol, while for a charged cluster (-6 , to account for the ionicity of the Cl atoms according to Mulliken charge analysis), N_2 has a binding energy of -0.12 kcal/mol. The calculation thus predicts that N_2 is quite free in the dipole well, facilitating the diffusion process.

The analysis above implies that the majority of the N atoms in the exposed part of the sample are in the form of initial NH_4^+ ions and photochemically formed N_2 molecules. From simple stoichiometry we have $2\text{NH}_4\text{Cl} \rightarrow \text{N}_2 + 8\text{H} + 2\text{Cl}$, that is, any other end product of the N_2 -forming reaction must be made up of Cl and H atoms only, with excess hydrogen that is probably released as hydrogen gas.

We find it probable that N_2 formation is efficient also in other ammonium halides, as we see the signal associated with the ammonium ion is decreasing in NH_4I (Figures 5 and 6a) at a rate which is much larger than for NH_4Cl . Most likely the depletion mechanisms are similar in the two halides, and the absence of N_2 signal suggests that the nitrogen molecules rapidly desorb from the sample or diffuse away from the probed volume. The iodide background signal is fairly constant in the initial phase due to the fact that the electrons associated with the iodine atoms totally dominate the cross section. The decrease in background at longer exposure is simply due to shadowing as a hole is formed in the sample.

The qualitative dose dependence of the FY intensity for NH_4Cl

is similar to that of NH_4Cl . A pronounced photon-induced N_2 peak increases with photon exposure while the signal corresponding to the initial chemical surrounding decreases. Ammonium phosphate is an adduct compound where the bonding between the NH_4 and PO_4H_2 groups is much less ionic than the bonding of NH_4^+ to the halogen ions in the ammonium halides. The observations show that the N_2 -forming mechanism as well as the tendency for the N_2 molecules to remain in the sample are not confined to ionic compounds and suggest that the mechanisms may be quite general. In the case of *l*-alanine, the dose dependence is much more complex, with spectral-shape changes throughout the spectrum, and here we find no evidence for N_2 formation.

Conclusions

Soft X-rays efficiently induce N_2 formation in NH_4Cl . The N_2 molecules are weakly bound in the sample and to a large extent remain in the exposed volume, especially at lower temperatures. Similar phenomena are expected in many different nitrogen compounds, especially where the atoms are tetrahedrally NH_4 coordinated. The results imply that neither catalyst nor high temperature is needed to form N_2 molecules in such compounds. We believe that this is possible because soft X-rays simultaneously excite electron–hole pairs and induce nuclear motion, which locally corresponds to high temperatures.

These results have direct implications for synchrotron radiation studies of complex nitrogen-containing compounds, where the probe itself may create structures, which can be mistakenly associated with the intact samples. We speculate that similar photochemical phenomena may also appear in complex carbon and oxygen compounds. The present type of investigations may be applied in catalysis, where in-situ studies⁵ are straightforward, using thin filters to separate vacuum and the interaction volume.

In addition, the results may have an impact on many fields where the balance between inert N_2 and more reactive nitrogen molecules is important. In the evolution of planetary atmospheres, and especially biospheres, this balance is essential. It is thought that the initial generation of N_2 in Earth's atmosphere is due to particles of frozen ammonia which form N_2 in stages of the planetary development with high temperature.¹ Direct formation of N_2 through ionizing radiation in nitrogen-containing dust is a possibility which may have been overlooked. The concentration of NH_3 as well as NH_4^+ in primitive Earth is known to be important for the synthesis of organic compounds,² and on the basis of the present results, we find it likely that the relative concentrations of these crucial species have been influenced by high-energy photons. The balance is also a present concern in environmental science and in connection with production of synthetic fertilizer.

Acknowledgment. This work was supported by the Swedish Science Council, the N3 Networking Activity of the European Community, and the Göran Gustafsson Foundation. We are grateful for the support by the staff of MAX-lab and BESSY.

References and Notes

- (1) Denlinger, M. C. *Earth, Moon, Planets* **2005**, 96, 59.
- (2) Bada, J. L.; Miller, S. L. *Science* **1968**, 159, 423.
- (3) Mulder, A. *Water Sci. Technol.* **2003**, 48, 67.
- (4) Weik, M.; Ravelli, R. B.; Kryger, G.; McSweeney, S.; Raves, M. L.; Harel, M.; Gros, P.; Silman, I.; Kroon, J.; Sussman, J. L. *Proc. Natl. Acad. Sci. U.S.A.* **2000**, 97, 623.
- (5) Mesu, J. G.; van der Eerden, Ad M. J.; de Groot, F. M. F.; Weckhuysen, B. M. *J. Phys. Chem. B* **2005**, 109, 4042.
- (6) Mesu, J. G.; Beale, A. M.; de Groot, F. M. F.; Weckhuysen, B. M. *J. Phys. Chem. B* **2006**, 110, 17671.

- (7) Patten, F. W.; Marrone, M. *J. Phys. Rev.* **1966**, *142*, 513.
- (8) Patten, F. W. *Phys. Rev.* **1968**, *175*, 1216.
- (9) Patten, F. W. *Solid State Commun.* **1968**, *6*, 65.
- (10) Marquardt, C. L.; Patten, F. W. *Solid State Commun.* **1969**, *7*, 393.
- (11) Aziz, E. F.; Freiwald, M.; Eisebitt, S.; Eberhardt, W. *Phys. Rev. B* **2006**, *73*, 075120.
- (12) Follath, R.; Senf, F. *Nucl. Instrum. Methods A* **2001**, *467*, 485.
- (13) Nordgren, J.; Bray, G.; Cramm, S.; Nyholm, R.; Rubensson, J.-E.; Wassdahl, N. *Rev. Sci. Instrum.* **1989**, *60*, 1690.
- (14) Denecke, R.; Väterlein, P.; Bässler, M.; Wassdahl, N.; Butorin, S.; Nilsson, A.; Rubensson, J.-E.; Nordgren, J.; Mårtensson, N.; Nyholm, R. *J. Electron Spectrosc. Relat. Phenom.* **1999**, *101*, 971.
- (15) Delley, B. *J. Chem. Phys.* **1990**, *92*, 508; Delley, B. *J. Chem. Phys.* **2000**, *113*, 7756, DMol is available from Accelrys.
- (16) Perdew, J. P.; Burke, K.; Ernzerhof, M. *Phys. Rev. Lett.* **1996**, *77*, 3865.
- (17) Monkhorst, H. J.; Pack, J. D. *Phys. Rev. B* **1976**, *13*, 5188.
- (18) Casida, M. E.; Daul, C.; Goursot, A.; Koester, A.; Pettersson, L. G. M.; Proynov, E.; St-Amant, A.; Salahub, D. R. *DEMON-KS*, version 4.0; deMon Software, 1997.
- (19) Kutzelnigg, W.; Fleischer, U.; Shindler, M. *NMR—Basic Principles and Progress*; Springer-Verlag: Heidelberg, 1990; Vol. 23, p 165.
- (20) Chen, C. T.; Ma, Y.; Sette, F. *Phys. Rev. A* **1989**, *40*, 6737.
- (21) Glans, P.; Skytt, P.; Gunnelin, K.; Guo, J.-H.; Nordgren, J. *J. Electron Spectrosc. Relat. Phenom.* **1996**, *82*, 193.
- (22) Alavi, A.; Lynden-Bell, R. M.; Willis, P. A.; Swainson, I. P.; Brown, R. J. C. *Can. J. Chem.* **1998**, *76*, 1581.
- (23) Eisebitt, S.; Böske, T.; Rubensson, J.-E.; Eberhardt, W. *Phys. Rev. B* **1993**, *47*, 4103.
- (24) CXRO home page, http://www-cxro.lbl.gov/optical_constants/.
- (25) Waki, K.; Zhao, J.; Horikoshi, S.; Watanabe, N.; Hidaka, H. *Chemosphere* **2000**, *41*, 337.
- (26) O'Brien, W. L.; Jia, J.; Dong, Q.-Y.; Callcott, T. A.; Miyano, K. E.; Ederer, D. L.; Mueller, D. R.; Kao, C.-C. *Phys. Rev. B* **1993**, *47*, 140.
- (27) Rodebush, W. H.; Michalek, J. C. *J. Am. Chem. Soc.* **1929**, *51*, 748.
- (28) Holleman, A. F.; Wiberg E. *Lehrbuch der Anorganischen Chemie*; Walter de Gruyter: Berlin-New York, 1985.
- (29) Sandell, A.; Björneholm, O.; Nilsson, A.; Zdansky, E.; Tillborg, H.; Andersen, J. N.; Mårtensson, N. *Phys. Rev. Lett.* **1993**, *70*, 2000.
- (30) Björneholm, O.; Nilsson, A.; Sandell, A.; Hernnäs, B.; Mårtensson, N. *Phys. Rev. B* **1994**, *49*, 2001–2004.